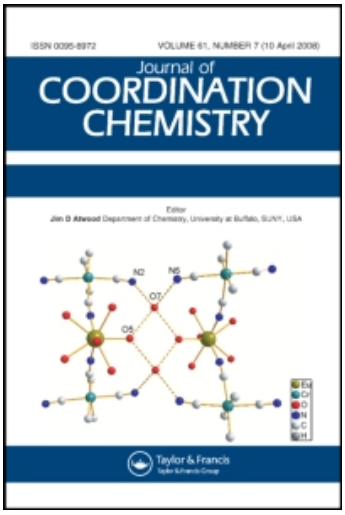

Journal of Coordination Chemistry
Publication details, including instructions for authors and subscription information:
http://www.informaworld.com/smpp/title~content=t713455674

The synthesis and thermal degradation products of the C-H bond activating complex [(diimine)Pt(Me)(OSO_2CF_3)]

Kjetil A. Netland[a]; Olivier Graziani[b]; Alexander Krivokapić[a]; Richard H. Heyn[b]; Mats Tilset[c]
[a] Department of Chemistry, University of Oslo, N-0315 Oslo, Norway [b] SINTEF Materials and Chemistry, N-0314 Oslo, Norway [c] Department of Chemistry, Centre for Theoretical and Computational Chemistry, University of Oslo, N-0315 Oslo, Norway

To cite this Article Netland, Kjetil A. , Graziani, Olivier , Krivokapić, Alexander , Heyn, Richard H. and Tilset, Mats(2009) 'The synthesis and thermal degradation products of the C-H bond activating complex [(diimine)Pt(Me)(OSO_2CF_3)]', Journal of Coordination Chemistry, 62: 19, 3085 — 3097
To link to this Article: DOI: 10.1080/00958970902991757
URL: http://dx.doi.org/10.1080/00958970902991757

Journal of Coordination Chemistry
Vol. 62, No. 19, 10 October 2009, 3085–3097

The synthesis and thermal degradation products of the C–H bond activating complex [(diimine)Pt(Me)(OSO_2CF_3)]

KJETIL A. NETLAND†, OLIVIER GRAZIANI‡, ALEXANDER KRIVOKAPIĆ†, RICHARD H. HEYN*‡ and MATS TILSET*§

†Department of Chemistry, University of Oslo, P. O. Box 1033 Blindern, N-0315 Oslo, Norway
‡SINTEF Materials and Chemistry, P. O. Box 124 Blindern, N-0314 Oslo, Norway
§Department of Chemistry, Centre for Theoretical and Computational Chemistry, University of Oslo, P. O. Box 1033 Blindern, N-0315 Oslo, Norway

(*Received 25 February 2009; in final form 3 April 2009*)

Design of a selective homogeneous methane functionalizing catalyst based on $[(ArN{=}CRCR{=}NAr)Pt(Me)(L)]^+$ requires knowledge of its stability in various reaction media, particularly water. Reaction of $(diimine)PtMe_2$ (**1**) (diimine = ArN=CRCR=NAr, Ar = 2, 6-$Me_2C_6H_3$, R = Me) with HOTf (OTf = OSO_2CF_3) gives the methane activating compound (diimine)Pt(Me)OTf (**3**). When varying amounts of H_2O are added during the synthesis of **3**, competing degradation pathways lead to two different characterizable products. With only trace amounts of water, two dimeric species, [(diimine)Pt(μ-Cl)(μ-OH)Pt(diimine)]$(OTf)_2$ (**6**) and [(diimine)Pt(μ-$OH)_2$Pt(diimine)]$(OTf)_2$ (**7**), are isolated, in addition to an uncharacterized dark brown precipitate. When an excess of H_2O is added, the aquo species [(diimine)Pt(Me)(H_2O)][OTf] (**5**) is first observed, which then reacts further to give a dark brown precipitate and **7**. The structures of **1**, **6**, and **7** are presented. Both **6** and **7** exhibit unusual conformations for their respective classes. Compound **6** has a rarely observed planar conformation, while **7** has an unusual bifurcated H-bonding motif between the bridging OH-groups and a triflate anion, with a highly bent conformation.

Keywords: Platinum; Structure; Methane activation

1. Introduction

A significant goal for the development of sustainable chemistry is the direct catalytic functionalization of light alkanes, such as methane, to oxygenates, such as methanol [1]. While homogeneous catalytic systems for such transformations exist, such as the Pt systems developed by Shilov [2] and Periana [3], unsuitable activities, co-reagents, or reaction conditions prevent the industrial implementation of these catalytic processes. The attack on this problem has led to a large amount of fundamental information on the activation of C–H bonds by transition metals, in particular Pt [4], and with

*Corresponding author. Email: Richard.H.Heyn@sintef.no; Mats.Tilset@kjemi.uio.no

ISSN 0095-8972 print/ISSN 1029-0389 online
DOI: 10.1080/00958970902991757

significant research on N-ligated Pt-methyl cations as models for the catalytic systems. This includes Pt species capable of activating methane under very mild conditions [5].

Design of a selective homogeneous methane functionalization catalyst based on $[(ArN{=}CRCR{=}NAr)Pt(Me)(L)]^+$ requires knowledge of its stability in various reaction media and studies to elucidate potential mechanistic pathways. In particular, the effect of water on these cations is important, since this is the preferred reaction solvent and/or source of OH, as in the Shilov cycle. Work from the Bercaw group has shown that $[(ArN{=}CRCR{=}NAr)Pt(R')(L)][BF_4]$ ($R = H, Me$; $R' = Me, Ph$; $L = CF_3CH_2OH, H_2O$) reacts cleanly with benzene up to three half-lives after which formation of the $(\mu\text{-}OH)_2$ dimer $[(ArN{=}CRCR{=}NAr_2)Pt_2(\mu\text{-}OH)_2][BF_4]_2$ starts *via* an unknown mechanism. The dimer formation is accelerated by higher Pt concentrations and retarded by adding water [6]. Herein, we present further studies on the stability of these Pt C–H activating complexes, in particular [(diimine)Pt(Me)(OTf)] (diimine = ArN=CRCR=NAr, Ar = 2,6-$Me_2C_6H_3$, R = Me; OTf = OSO_2CF_3), in the presence of H_2O. Two different degradation products have been obtained, depending on the amount of H_2O present.

2. Results and discussion

2.1. *Structure of (diimine)PtMe$_2$ (1)*

Compound **1**, (diimine)$PtMe_2$, is the starting complex for the synthesis of the cationic C–H activating complexes [7], but its structure has never been reported. Dark purple crystals of **1** suitable for X-ray diffraction analysis were obtained by slow evaporation of a dichloromethane solution at room temperature. An ORTEP drawing [8] of the structure is shown in figure 1. Pertinent bond distances and angles are given in table 1.

The structure confirms that the complex is monomeric and contains a κ^2-(N,N)-chelating diimine. The molecular geometry is square-planar as expected for a four-coordinated d^8 species; the sum of the four *cis* L–Pt–L′ angles is 360.0°. Deviations from the ideal 90° L–Pt–L′ angle are however considerable, ranging from 76.16(8)° for the N(1)–Pt–N(2) chelate bite angle, to 98.15(10)° for the N(2)–Pt–C(22) angle. These observations are consistent with previous structural studies on functionalized diimine (κ^2-N,N)$PtMe_2$ complexes [9].

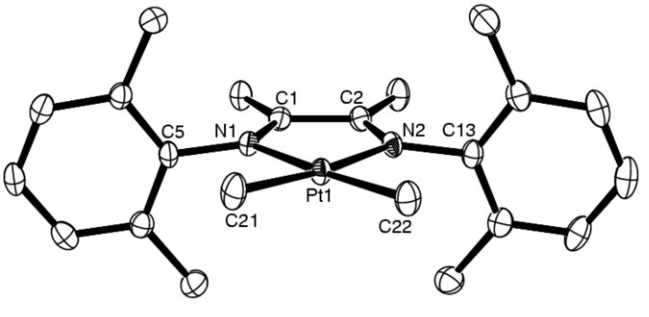

Figure 1. ORTEP drawing of **1** with 50% probability ellipsoids. H-atoms removed for clarity.

The structure of **1** can be compared to the structure of the nearly identical diimine-chelated platinum compound (diimine)$PtPh_2$ (**2**) [10]. The C=N bond lengths are practically identical in both two compounds, however, slight differences are observed in the structural environment around Pt(II). First, the Pt–C bond length (average 2.042 Å) in **1** is slightly longer than the corresponding average distance found in **2** (average 2.010 Å), in accordance with the increase in M–C bond strength from the M–C(sp^3) bond in **1** to the M–C(sp^2) bond in **2** [11]. Second, a slight shortening of the Pt–N bond distances is seen in **1** (average 2.083 Å) as compared to **2** (average 2.104 Å), which is in accordance with weaker *trans* influence of the methyl ligand relative to the phenyl group. In comparison with the previously reported crystal structure of the free diimine [12], a slight elongation of both the N–C(aryl) and the imine C=N bond (0.02 Å) is observed upon coordination of the diimine to Pt. This trend is consistent with a small decrease in the bond order of the imine C=N double bond, a consequence of the d(π)–p(π) back bonding from Pt to N.

2.2. *Synthesis of [(diimine)Pt(Me)(OTf)] (3)*

Protonolysis of **1** in dichloromethane with one equivalent HOTf provides [(diimine)Pt(Me)(OTf)] (**3**) (scheme 1). While **3** could not be isolated and was unstable in poorly coordinating solvents at ambient temperature, an *in situ* synthesis in dichloromethane-d_2 confirmed that **3** was indeed the major product, based on comparison of its ^{1}H NMR spectrum to the previously characterized, closely related triflate complex [(ArN=CRCR=NAr)Pt(Me)(OTf)] (Ar = 3,5-$(CF_3)_2C_6H_3$, R = Me) (**4**) [13]. In particular, the ^{1}H NMR spectrum showed a new singlet at δ 0.85 and flanked by ^{195}Pt satellites ($^2J(^{195}Pt–H) = 75.0$ Hz), which is slightly downfield and with a smaller

Table 1. Bond distances (Å) and angles (°) for **1**.

Pt(1)–N(1)	2.078(2)	Pt(1)–N(2)	2.088(2)
Pt(1)–C(21)	2.036(3)	Pt(1)–C(22)	2.048(3)
N(1)–C(1)	1.296(3)	N(1)–C(5)	1.443(3)
N(2)–C(2)	1.293(4)	N(2)–C(13)	1.440(3)
C(1)–C(2)	1.486(4)		
N(1)–Pt(1)–N(2)	76.16(8)	N(1)–Pt(1)–C(21)	96.91(10)
N(1)–Pt(1)–C(22)	174.29(9)	N(2)–Pt(1)–C(21)	172.50(10)
N(2)–Pt(1)–C(22)	98.15(10)	C(21)–Pt(1)–C(22)	88.76(11)

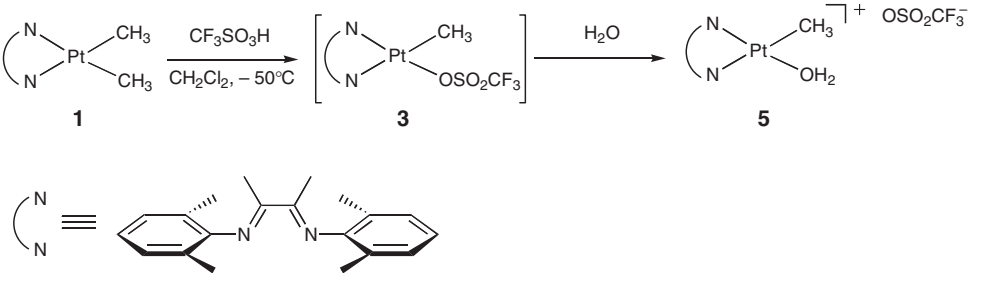

Scheme 1. Synthesis of Pt complexes **3** and **5**.

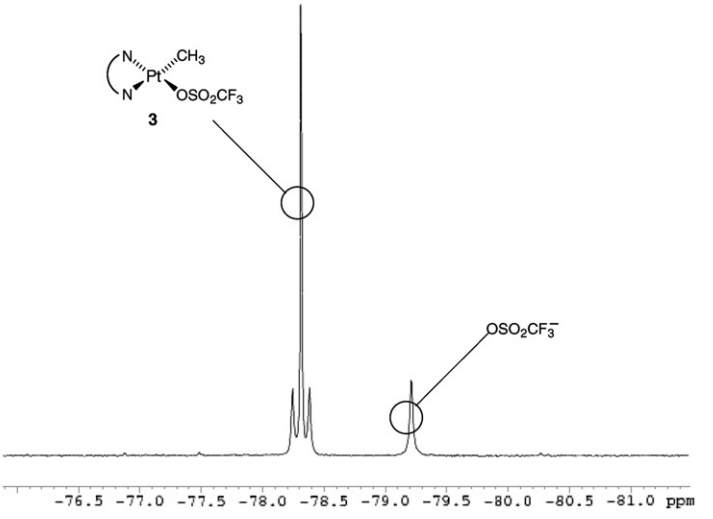

Figure 2. Selected part of the ^{19}F NMR spectra showing the covalently bonded triflate complex **3** and minor amounts of free triflate. The intensity of the latter increases with time due to decomposition of **3**.

J value than that of the corresponding Pt–Me resonance for **1** (δ 0.81, $^2J(^{195}Pt–H) =$ 86.5 Hz) [14]. In the ^{19}F NMR spectrum, a singlet was observed at δ 78.3 with ^{195}Pt satellites ($^4J(^{195}Pt–F) = 13$ Hz), demonstrating that the triflate group is covalently bonded to the Pt (figure 2). Observation of $^{195}Pt–F$ coupling in Pt–OTf complexes is definitive for determining the existence of a covalently bonded solution structure [5, 13], which can be difficult to ascertain from other spectroscopic methods [15]. The thermal stability of **3** at ambient temperature was qualitatively determined from monitoring of the ^1H and ^{19}F NMR spectra of freshly prepared compound **3**. After 13 h, the ^{19}F NMR signal of **3** had decreased to *ca* one-fourth of its original intensity, and this change was accompanied by methane liberation and formation of a dark brown precipitate. These observations are comparable to those for **4**, although its degradation occurred over a somewhat longer period [13].

2.3. *Thermal degradation of [(diimine)Pt(Me)(OTf)] in the presence of H_2O*

While the dark brown precipitate resulting from the thermal instability of **3** in dichloromethane could not be characterized, careful addition of varying amounts of water to the protonolysis reaction of **1** provided insight into the degradation pathways of **3**. When HOTf containing only adventitious water was used for the protonolysis, and the resulting reaction heated at 35°C for 1 week, a mixture of yellow (major) and red crystals, as well as some dark brown precipitate, was obtained. The darkish precipitate could be removed by washing with dichloromethane, but separation of the yellow and red crystals was only possible manually with the aid of a microscope. If instead the protonolysis of **1** was conducted with *ca* five equivalents of H_2O, a dark red solution of the aqua complex [(diimine)Pt(Me)(H_2O)][OTf] (**5**) was initially obtained [16]. Reduction of the volume under argon and subsequent heating of the reaction at 40°C for several days resulted in the darkening of the solution and the exclusive formation of red crystals.

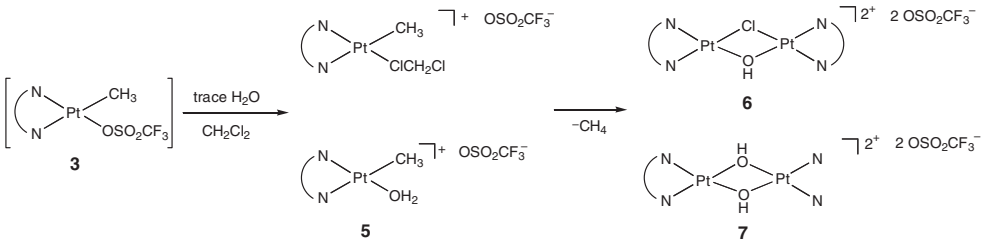

Scheme 2. Thermal degradation of **3** with substoichiometric amounts of H_2O.

Structural characterization of the yellow crystals formed in the former reaction (the upper pathway in scheme 2) identified the complex to be the unusual mixed bridging species $[(diimine)_2Pt_2(\mu\text{-}OH)(\mu\text{-}Cl)][OTf]_2$ (**6**). The red crystals from the latter reaction (the lower pathway in scheme 2) were found by X-ray crystallography to be the hydroxyl-bridged dimer $[(diimine)Pt(\mu\text{-}OH)]_2[OTf]_2$ (**7**). While a slight increase of water was necessary to obtain a reasonable yield of **7**, greater amounts of water lowered the yield. The red crystals formed as a secondary product in the upper pathway in scheme 2 were identified as **7** by comparison of the MS data for each set of crystals.

The formation of two distinct products when only trace amounts of H_2O are present during the protonolysis of **1** to provide **3**, suggests that competing degradation pathways are involved, the choice of which will depend on the concentration and binding affinities of the different potentially coordinating molecules involved. In this case, the competing pathways most likely involve the displacement of the coordinated triflate in **3** by either CH_2Cl_2 or H_2O. While this is confirmed for a stoichiometric excess of the better coordinating ligand H_2O, *via* the identification of **5**, the proposed intermediate species for the other pathway, $[(diimine)Pt(Me)(ClCH_2Cl)]^+$, was unobserved. A corresponding irreversible C–Cl bond activation to form a mono Cl-bridged dimer has, however, been reported when the solvent-coordinated Re cations $[Re(CO)_4(PR_3)(CH_2Cl_2)]^+$ ($R = Ph, {}^iPr, Cy$) are exposed to H_2O [17], and the related dimer $[(diimine)Pt(\mu\text{-}Cl)_2]_2[BF_4]_2$ was synthesized from $[(diimine)Pt(\mu\text{-}OH)_2]_2[BF_4]_2$ in CH_2Cl_2, again with the solvent the apparent source of Cl [18].

The dinuclear complexes **6** and **7** were poorly soluble in the weakly coordinating solvent dichloromethane. In the more polar solvents like acetonitrile, nitromethane, and methanol, NMR spectra indicated reaction of **7** with these solvents, the products of which have not yet been identified. Given the low solubility of **7**, it was not possible to get a satisfactory ^{13}C NMR spectrum, thus the ^{13}C NMR data were derived from HMQC and HMBC spectra. The formation of a Cl-bridge in **6** was supported by MS/HRMS data obtained from acetonitrile solutions of **6**. In these experiments, the acetonitrile adduct $(diimine)Pt^{194}(Cl)(CH_3CN)^+$ ($m/z = 562.1504$) dominated the fragmentation pattern. The mass peak of a corresponding monomer was not observed in the ESI-MS spectrum **7**; in this case, the parent ion of dicationic **7** ($m/z = 503.1567$) dominated the mass spectrum.

2.4. *Structure of [(diimine)Pt(μ-Cl)(μ-OH)Pt(diimine)](OTf)₂ (6)*

An ORTEP drawing of **6** is shown in figure 3 and relevant bond distances and angles are given in table 2. The structure of **6** consists of two edge-sharing square planar

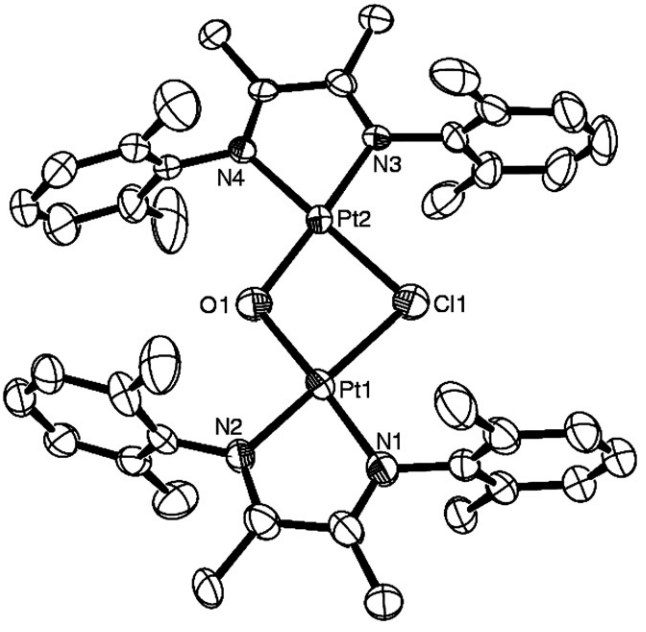

Figure 3. ORTEP drawing of **6** with 40% probability ellipsoids. Hydrogen atoms, triflate anions, and solvent of crystallization have been removed for clarity.

Table 2. Bond distances (Å) and angles (°) for **6**.

Pt(1)–Cl(1)	2.317(3)	Pt(1)–O(1)	2.010(7)
Pt(1)–N(1)	1.978(7)	Pt(1)–N(2)	1.974(6)
Pt(2)–Cl(1)	2.316(3)	Pt(2)–O(1)	2.021(7)
Pt(2)–N(3)	1.965(6)	Pt(2)–N(4)	1.981(6)
Cl(1)–Pt(1)–O(1)	82.4(2)	Cl(1)–Pt(1)–N(1)	100.8(2)
Cl(1)–Pt(1)–N(2)	179.3(2)	O(1)–Pt(1)–N(1)	176.8(3)
O(1)–Pt(1)–N(2)	97.1(3)	N(1)–Pt(1)–N(2)	79.6(3)
Cl(1)–Pt(2)–O(1)	82.2(2)	Cl(1)–Pt(2)–N(3)	100.9(2)
Cl(1)–Pt(2)–N(4)	178.4(2)	O(1)–Pt(2)–N(3)	176.1(3)
O(1)–Pt(1)–N(4)	97.5(3)	N(3)–Pt(2)–N(4)	79.5(3)
Pt(1)–Cl(1)–Pt(2)	88.30(10)	Pt(1)–O(1)–Pt(2)	106.4(3)

Pt moieties, bridged by Cl and OH. There is a very small deviation in the Pt1, N1, N2, Cl1, O1 least-squares plane, with the maximum deviation of only 0.006 Å, while the other plane is slightly more distorted, with a maximum distance from the least-squares plane of 0.04 Å. The core of the dimer is nearly planar, as the bending angle between the two square planes is only 172.1°. Dinuclear dications and triflate anions are associated in the solid state by a number of hydrogen bonds primarily involving the Me groups of the diimine ligands and the oxygen atoms of the triflate anions. The hydrogen of the bridging OH was not located. This, and the lack of any H-bonding to the OH, makes it impossible to determine if the H-atom is within or bent out of the planar Pt_2ClO core.

The Pt–Cl1 bonds have essentially the same length, 2.317(3) Å, while the Pt1–O1 bond of 2.010(7) Å is slightly shorter than Pt2–O1 bond of 2.022(8) Å. All the Pt–N

distances are within 0.01 Å of the average distance of 1.975 Å. The Pt–N distances are measurably shorter than 2.083 Å, the average Pt–N distance in **1**, consistent with the poorer *trans* influence of Cl^- and OH^- compared to Me^-, in addition to different electrostatic effects between neutral **1** and cationic **6**. Otherwise, all the bonding distances are similar to those reported for other dicationic diimine-containing Pt dimers with a bridging Cl or OH *trans* to a diimine nitrogen [18]. The Pt–Pt distance is 3.227 Å, intermediate between the Pt–Pt distances in planar $[(ArN{=}CRCR{=}NAr)Pt(\mu\text{-}Cl)]_2[BF_4]_2$ ($Ar = 4\text{-}MeC_6H_4$, R = Me) and planar $[(ArN{=}CRCR{=}NAr)Pt(\mu\text{-}OH)]_2[BF_4]_2$ ($Ar = 4\text{-}^tBuC_6H_4$, R = Me) (**8**) [18]. All the *cis* L–Pt–L′ angles around Pt deviate significantly from 90°. In addition to the expected acute N–Pt–N angles, which are 79.5°, the average Cl1–Pt–O1 angle is 82.3°, which increases the *cis* O1–Pt–N and Cl1–Pt–N angles to 97.3 and 100.8°, respectively. The Pt1–Cl1–Pt2 angle is 88.3(1)°, and the Pt1–O1–Pt2 angle is 106.4(3)°. All these values compare well with similar values in the other two structurally characterized mixed bridging (μ-OH)(μ-Cl) edge-sharing binuclear d^8 compounds [19].

Compound **6** is the first structurally characterized example of a mixed (μ-OH)(μ-Cl) bridged Pt complex, although there are a few structurally characterized Pt dimers with mixed (μ-ER)(μ-Cl) bridges (E = S, Se, Te) [20]. Pt dimers with mixed (μ-OR)(μ-Cl) bridges (R = H or Me) have been reported, but not structurally characterized [21]. For edge-sharing binuclear d^8 compounds, structurally characterized dimers containing mixed bridging ligands are relatively unusual; the vast majority have (μ-Cl)(μ-SR) bridges. In addition to the two (μ-OH)(μ-Cl) dimers, the structure of a Pd-based (μ-OH)(μ-Br) dimer is known [22]. As confirmed computationally [23], a bent structure is the norm for this class of compounds. Thus, the planar structure of **6** is unusual, and **6** is one of only a handful of compounds in this class to have this structure [20d, 24].

2.5. *Structure of [(diimine)Pt(μ-OH)$_2$Pt(diimine)](OTf)$_2$ (7)*

An ORTEP drawing of **7** is shown in figure 4. Selected bond distances and angles are given in table 3. Like **6**, the structure of **7** consists of two edge-sharing, square-planar Pt moieties, but in this case they are bridged by two OH-groups. As in **6**, one square plane (O1, O2, Pt2, N3, and N4) shows little deviation from planarity (average 0.006 Å), while the other square plane shows slightly more deviation (average distance from the least squares plane is 0.036 Å). The metrical parameters around each Pt in **7** are also generally quite similar to those in **6**, except for slight changes in some of the *cis* angles involving the bridging atoms, a consequence of the shorter Pt–O bond distances in **7** as compared to the corresponding Pt–Cl distances in **6**. In particular, the O–Pt–O angles are slightly smaller than the O–Pt–Cl angles in **6**, with a corresponding slight increase in the *cis* O–Pt–N angles *versus* the Cl (or O)–Pt–N angles in **6**.

In contrast to planar **6**, the overall structure of **7** has a clear bent *exo* conformation [23], with a bending angle between the two square planes of 141.6°, and the hydrogens pointing away from the metal centers. This bending reduces the Pt–Pt distance from 3.227 Å in **6** to 2.982 Å and reduces the Pt–O–Pt angle from 106.4° in **6** to 94.1° (average) in **7**. The bending is manifested by the unusual bifurcated H-bonding between the bridging OH and two distinct oxygens of one triflate anion, which is situated directly over one half of the Pt_2O_2 dimer. Indeed, the Pt1–Pt2–S1–C41 torsion angle is only 4.8°. While this bifurcated H-bonding motif has been observed in monomeric

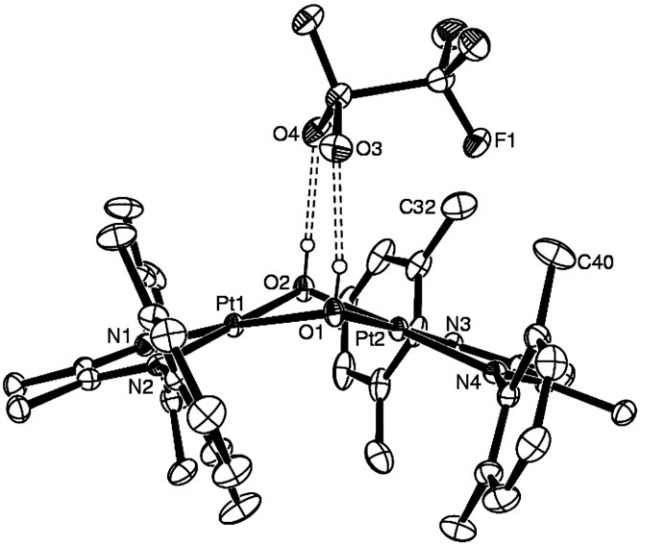

Figure 4. ORTEP drawing of **7**, with 30% probability ellipsoids. All non-hydrogen bonding hydrogen atoms, the non-hydrogen bonding triflate anion, and H_2O of crystallization removed for clarity. The dashed bonds indicate the hydrogen bonding interactions.

Table 3. Selected bond distances (Å) and angles (°) for **7**.

Pt(1)–O(1)	2.043(3)	Pt(1)–O(2)	2.028(3)
Pt(1)–N(1)	1.990(4)	Pt(1)–N(2)	1.987(4)
Pt(2)–O(1)	2.047(3)	Pt(2)–O(2)	2.033(3)
Pt(2)–N(3)	1.970(4)	Pt(2)–N(4)	1.980(4)
O(1)···O(3)	2.806(9)	O(2)···O(4)	2.861(9)
O(1)–Pt(1)–O(2)	79.44(13)	N(1)–Pt(1)–N(2)	78.99(16)
O(1)–Pt(1)–N(1)	175.43(15)	O(2)–Pt(1)–N(2)	178.69(14)
O(1)–Pt(1)–N(2)	101.83(14)	O(2)–Pt(1)–N(1)	99.72(14)
O(1)–Pt(2)–O(2)	79.24(13)	N(3)–Pt(2)–N(4)	78.94(15)
O(1)–Pt(2)–N(4)	102.44(14)	O(2)–Pt(2)–N(3)	99.36(14)
O(1)–Pt(2)–N(3)	178.36(14)	O(2)–Pt(2)–N(4)	177.94(14)
Pt(1)–O(1)–Pt(2)	93.59(13)	Pt(1)–O(2)–Pt(2)	94.49(13)

bis-aquo complexes [25], it is highly unusual, if not unique, in *bis*(μ-OH) dimers. The O1–O2 distance is 2.600 Å, which is very close to the distance of 2.43 Å between the H-bonding acceptors O3 and O4 of the triflate anion. In addition to the H-bonding between the bridging OHs of the dimer and the O3 and O4 of the triflate, there are short contacts between F1 of the triflate anion and the *ortho* Me groups C32 and C40 of the diimine 2,6-dimethylphenyl group.

Two other structures closely related to **7**, $[(ArN{=}CRCR{=}NAr)Pt(\mu\text{-}OH)]_2[BF_4]_2$ (Ar = 3,5-^{t}Bu$_2$C$_6$H$_3$, R = Me) [26] and **8**, are both planar. The former has a planar, *anti* conformation due to H-bonding between the bridging OH groups and two THF molecules of crystallization, one above and one below the Pt_2O_2 plane, while the latter has no H-bonding interactions. Despite the difference in conformation, the metrics for all three of these structures are essentially the same, except for the Pt–O–Pt angle, which

is reduced from about 101° in the planar structures to 94.1° (average) in **7**, and the Pt–Pt distance, which is reduced from about 3.14 to 2.982 Å. Curiously, the related Pd dimer $[(ArN{=}CRCR{=}NAr)Pd(\mu\text{-}OH)]_2[BF_4]_2$ ($Ar = 4\text{-}MeOC_6H_4$, R = Me), which has no H-bonding interactions involving the bridging OH, is also bent, with a bending angle and metric parameters very close to those of **7** [18]. This difference is observed despite that weak metal–metal interactions, which can be a driving force for bending, have approximately the same strength for Pd and Pt [23].

A theoretical analysis for the preference of planar or bent edge-sharing d^8 dimers of the form $M_2(\mu\text{-}XR)_2L_4$ shows that small energy differences resulting from electronic, steric, or packing effects can lead to the stability of one conformer over another [23]. A comparison of the known structures for the general class of $[(NN)Pt(\mu\text{-}OH)]_2^{2+}$ dimers (NN = bipyridine and phenanthroline-based ligands) shows that the vast majority have planar structures [27] and exhibit some sort of H-bonding between the bridging OH-groups and another structural unit (anion, solvent of crystallization, or another dimer). The only known bent structures are $[(DPK)Pt(\mu\text{-}OH)]_2[OTf]_2$ (DPK = di-2-pyridyl ketone) [28], with a bending angle of 152.5° and $[(Me_2phen)Pt(\mu\text{-}OH)_2][OTf]_2$ **9** (Me_2phen = 2,9-dimethyl-1,10-phenanthroline) [29], which has an angle of 136.9°. In the former complex, the bent dimer is associated *via* H-bonding through OTf^- to a second, planar dimer (one OTf^- on each side of the dimer pair), suggesting that the bending is a result of some undetermined crystal packing forces. In the latter complex, the bending is claimed to be associated with the relief of steric interactions between the Me groups and bridging OH, since the corresponding non-methylated complex has a planar structure [27b]. Comparison of **7** and **9** shows that while the O–Pt–O angle in **7** is bit larger (79.3 *vs.* 77.3°), the Pt–O–Pt angle is smaller (94.1 *vs.* 96.4°) and the Pt–Pt distances and O–O distances in **7** are shorter (2.982 *vs.* 3.022 Å and 2.600 *vs.* 2.72 Å, respectively). Based on the examples discussed above, it does not seem possible to determine whether the unique H-bonding between the bridging OH-groups and the triflate anion is the cause or the consequence of the unusual bending conformation of **7**.

3. Conclusion

The methane activating species [(diimine)[Pt](Me)(OTf)] is thermally sensitive, degrading at ambient temperature to yield primarily an uncharacterized dark brown material. However, careful regulation of the amount of water and the temperature of reaction allows isolation of two distinct degradation products. With only trace amounts of water, two different dimeric species, $[(diimine)Pt(\mu\text{-}Cl)(\mu\text{-}OH)Pt(diimine)](OTf)_2$ (**6**) and $[(diimine)Pt(\mu\text{-}OH)_2Pt(diimine)](OTf)_2$ (**7**) are isolated, in addition to the dark brown precipitate. When an excess of H_2O is added, decomposition gives only the dark brown precipitate and the compound **7**. The formation of two different degradation products suggests the presence of competitive degradation pathways dependent on the nature of any available, potentially coordinating molecules. Compound **6** probably arises from coordination of the CH_2Cl_2 solvent, suggesting that other decomposition pathways may be accessible with other solvents.

The structures of both the decomposition products are unusual. Compound **6** is the first example of a Pt-containing, (μ-Cl)(μ-OH) edge-sharing dimer. While mixed

(μ-Cl)(μ-ER) bridged dimers generally have bent conformations, **6** has a rarely observed planar structure. On the other hand, the (μ-OH)$_2$ dimer **7** has an unusual bent conformation, exhibiting a unique bifurcated H-bonding motif between the bridging OH-groups and two O atoms of a triflate anion situated directly over half of the Pt_2 dimer. The causal relationship between the bent conformation and the H-bonding motif cannot, however, be determined.

4. Experimental

4.1. *General comments*

All reactions involving organometallic compounds were carried out under argon with Schlenk techniques. Solvents for reactions and NMR studies were dried according to standard procedures. NMR spectra were recorded at 25°C on a Bruker Avance DPX200 instrument with a QNP probe (^{1}H, ^{13}C, and ^{19}F) or a DRX 500 instrument with a TXI probe (^{1}H). Some ^{13}C NMR data were derived from HMQC and HMBC spectra. Assignments of ^{1}H and ^{13}C signals were aided by HMQC, HMBC, and COSY45. Chemical shifts are reported in ppm and referenced to either solvent (^{1}H and ^{13}C) or $CFCl_3$ (^{19}F). All J values are reported in Hz. Mass spectra (electrospray ionization) were obtained from acetonitrile solutions on a Micromass QTOF II spectrometer. Elemental analyses were preformed by Ilse Beetz Mikroanalytisches Laboratorium, Kronach, Germany.

4.2. *Synthesis of compounds*

4.2.1. Preparation of (diimine)Pt(CH_3)(OTf) (3). Triflic acid (1.4 μL, 0.016 mmol) was added under Ar to a Young NMR tube containing a solution of **1** (8.5 mg, 0.016 mmol) in dichloromethane-d_2 (0.5 mL) at −50°C. The resulting dark red mixture was warmed to ambient temperature, during which the color gradually changed to dark brown. NMR analysis after warming showed that the compound **3** was the major product. δ_H (200 MHz; CD_2Cl_2) 0.85 (3H, s, ^2J(^{195}Pt–H) 75.0, $PtCH_3$), 1.51 (3H, s, ^4J(^{195}Pt–H) 13.3, N=CCH_3), 1.79 (3H, s, N=CCH_3), 2.22 (6H, s, ArCH_3), 2.29 (6H, s, ArCH_3), 7.0–7.2 (6H, m, ArH); δ_F (188 MHz; CD_2Cl_2) 78.3 (3F, s, ^4J(^{195}Pt–F) 13.0, SO_3CF_3).

4.2.2. Preparation of a mixture of [(diimine)$_2$Pt$_2$(μ-OH)(μ-Cl)][OTf]$_2$ (6) and [(diimine)Pt(μ-OH)]$_2$[OTf]$_2$ (7). An ampoule loaded with **1** (33.4 mg, 0.0645 mmol) in dry CH_2Cl_2 (1.5 mL) was frozen in an inert atmosphere. Non-dried, 99% triflic acid (5.5 μL, 0.062 mmol) was added to the frozen solution before the ampoule was sealed under vacuum. The sealed ampoule was transferred to a cold bath (−50°C) and slowly warmed to room temperature. The reaction was then heated to 35°C for 1 week, providing a crystalline mixture of **6** (yellow, major component) and **7** (red, minor component). The crystals (11 mg, 26% combined yield) were washed with several portions of CH_2Cl_2. Individual samples for spectroscopic and crystallographic characterization of each product were obtained by physical separation of the yellow and red crystals under a microscope. ESI-MS analysis of the red crystals gave identical

data to those reported for **7**. The ESI-MS spectrum for yellow crystals of **6** showed peaks arising from monometallic fragments only, in particular the diagnostic acetonitrile adduct (diimine)Pt(Cl)$(NCCH_3)^+$; *m/z* (ESI) 563.2 ($[M(^{195}Pt)]^+$, 95%), 562.2 ($[M(^{194}Pt)]^+$, 62%); *m/z* (HR-ESI) 562.1514 ($C_{22}H_{27}N_3Cl^{194}Pt^+$ requires 562.1504).

4.2.3. Preparation of [(diimine)Pt(μ-OH)]$_2$[OTf]$_2$ (7). Water (9.2 µL, 0.51 mmol) was added to **1** (52.9 mg, 0.102 mmol) in CH_2Cl_2 (6.5 mL). The solution was cooled to −40°C before triflic acid (9.0 µL, 0.10 mmol) was added. The mixture was allowed to warm to room temperature over 24 h. The volume was reduced to one fifth under argon and the reaction mixture heated in a sealed tube at 40°C for several days giving the product as red crystals. The crystals (24 mg, 36%) were washed with several portions of CH_2Cl_2 (Found (%): C, 37.5; H, 4.1; N, 4.0. Calcd for $C_{42}H_{50}F_6N_4O_8S_2Pt_2 \cdot H_2O$ (%): C, 38.1; H, 4.0; N, 4.23). δ_H (500 MHz; CD_2Cl_2) 1.92 (12 H, s, N=CCH_3), 2.23 (24 H, s, ArCH_3), 7.08–7.09 (8H, m, *meta*-C_6H_5), 7.13–7.16 (4H, m, *para*-C_6H_5); δ_C (500 MHz; CD_2Cl_2) 17.4 (N=C*C*), 18.7 (ArCH_3), 129.0 (*meta*-C), 129.5 (*para*-C), 141.2 (*ortho*-C), 141.3 (*ipso*-C), 180.4 (C=N); *m/z* (EI) 504.2 ($[M(^{195}Pt/^{195}Pt)]^{2+}$, 100%), 503.7 ($[M(^{195}Pt/^{194}Pt)]^{2+}$, 57%), 503.2 ($[M(^{194}Pt/^{194}Pt)]^{2+}$, 18%); *m/z* (HR-EI) 503.1567 ($C_{40}H_{50}N_4O_2{}^{194}Pt_2{}^{2+}$ requires 503.1588).

4.3. *X-ray crystallography*

Pertinent parameters for data collection and refinement for all compounds are provided in table 4. The crystals were mounted on glass fibers with perfluoropolyether, and the data collected at 105 K on a Siemens 1 K SMART CCD diffractometer using graphite-monochromated Mo-Kα radiation. Data collection method: ω-scan, range is 0.3°, crystal to detector distance is 5 cm. Data reduction and cell determination were carried out with the SAINT and XPREP [31] programs. Absorption corrections were applied by using the SADABS program (G.M. Sheldrick, Private communication, 1996). All structures were solved using the Sir92 program [32], and refined on *F* using the program

Table 4. Crystal data and refinement parameters for **1**, **6**, and **7**.

	1	**6** · 0.5CH_2Cl_2	**7** · H_2O
Formula	$C_{22}H_{30}N_2Pt$	$C_{42.5}H_{49}Cl_2F_6N_4O_7Pt_2S_2$	$C_{42}H_{52}F_6N_4O_9Pt_2S_2$
Weight	517.58	1366.08	1325.20
System	Monoclinic	Monoclinic	Monoclinic
Space group	$P2_1/c$	$C2/c$	$P2_1/c$
Unit cell dimensions (Å, °)			
a	19.941(2)	41.979(3)	20.5276(9)
b	7.2806(8)	11.7797(8)	12.2143(5)
c	14.0975(15)	22.0358(13)	21.3137(9)
β	99.220(2)	114.0520(10)	111.6730(10)
V (Å^3)	2020.3(4)	9950.5(11)	4966.2(4)
Z	4	4	4
Total reflections	18,593	31,404	45,789
R_1 (all data)	0.0226	0.0995	0.0437
wR_2 (all data)	0.0247	0.0669	0.0510

Crystals [33]. The non-hydrogen atoms were refined with anisotropic thermal parameters; all hydrogens were located in a difference map, but those attached to carbon were repositioned geometrically. The H atoms were initially refined with soft restraints on the bond lengths and angles to regularize their geometry (C–H distances in the range 0.93–0.98 Å) and isotropic adsorptions (U(H) in the range 1.2–1.5 × U_{equiv} of the adjacent atom), after which they were refined with riding constraints.

Supplementary material

Crystallographic data for **1**, **6**, and **7** have been deposited with the Cambridge Crystallographic Data Center and are available free of charge under the CCDC numbers 716570, 716571, and 716572, respectively.

Acknowledgements

We gratefully acknowledge the generous support of the Norwegian Research Council, *via* post-doctoral stipends to O. G. R. (project number 151727/431) and A. K. (project number 160286/V30), and the Department of Chemistry, University of Oslo (stipend to K. A. N.).

References

[1] H. Arawaka, M. Aresta, J.N. Armor, M.A. Barteau, E.J. Beckman, A.T. Bell, J.E. Bercaw, C. Creutz, E. Dinjus, D.A. Dixon, K. Domen, D.L. DuBois, J. Eckert, F. Fujita, D.H. Gibson, W.A. Goddard, D.W. Goodman, J. Keller, G.J. Kubas, H.H. Kung, J.E. Lyons, L.E. Manzer, T.J. Marks, K. Morokuma, K.M. Nichols, R. Periana, A. Que, J. Rostrup-Nielson, W.M.H. Sachtler, L.D. Schmidt, A. Sen, G.A. Somorjai, P.C. Stair, B.R. Stults, W. Tumas. *Chem. Rev.*, **101**, 953 (2001).
[2] N.F. Goldshlegger, V.V. Eskova, A.E. Shilov, A.A. Shteinman. *Zh. Fiz. Khim.*, **46**, 1353 (1972).
[3] R.A. Periana, D.J. Taube, S. Gamble, H. Taube, T. Satoh, H. Fujii. *Science*, **280**, 560 (1998).
[4] M. Lersch, M. Tilset. *Chem. Rev.*, **105**, 2471 (2005).
[5] L. Johansson, O.B. Ryan, M. Tilset. *J. Am. Chem. Soc.*, **121**, 1974 (1999).
[6] H.A. Zhong, J.A. Labinger, J.E. Bercaw. *J. Am. Chem. Soc.*, **124**, 1378 (2002).
[7] L. Johansson, M. Tilset. *J. Am. Chem. Soc.*, **123**, 739 (2001).
[8] L.J. Farrugia. *J. Appl. Cryst.*, **30**, 565 (1997).
[9] (a) L. Johansson, O.B. Ryan, C. Rømming, M. Tilset. *Organometallics*, **17**, 3957 (1998); (b) K. Yang, R.J. Lachicotte, R. Eisenberg. *Organometallics*, **17**, 5102 (1998).
[10] B.J. Wik, M. Lersch, A. Krivokapic, M. Tilset. *J. Am. Chem. Soc.*, **128**, 2682 (2006).
[11] H.E. Bryndza, L.K. Fong, R.A. Paciello, W. Tam, J.E. Bercaw. *J. Am. Chem. Soc.*, **109**, 1444 (1987).
[12] N. Kuhn, M. Steimann, I. Walker. *Z. Kristallogr. – New Cryst. Struct.*, **216**, 319 (2001).
[13] H. Heiberg, L. Johansson, O. Gropen, O.B. Ryan, O. Swang, M. Tilset. *J. Am. Chem. Soc.*, **122**, 10831 (2000).
[14] L. Johansson. Hydrocarbon C-H activation of cationic Pt(II) diimine complexes, PhD thesis, University of Oslo (2000).
[15] (a) W. Beck, K. Sünkel. *Chem. Rev.*, **88**, 1405 (1988); (b) S.H. Strauss. *Chem. Rev.*, **93**, 927 (1993).
[16] The BF_4-salt of this cation has been characterized. L. Johansson, M. Tilset, J.A. Labinger, J.E. Bercaw. *J. Am. Chem. Soc.*, **122**, 10846 (2000).
[17] J. Huhmann-Vincent, B.L. Scott, G.J. Kubas. *Inorg. Chem.*, **38**, 115 (1999).
[18] S. Kannan, A.J. James, P.R. Sharp. *Polyhedron*, **19**, 155 (2000).

[19] These are bent, Pd(II) dimers. (a) C.-L. Chen, Y.-H. Liu, S.-M. Peng, S.-T. Liu. *J. Organomet. Chem.*, **689**, 1806 (2004); (b) A. Apfelbacher, P. Braunstein, L. Brissieux, R. Welter. *Dalton Trans.*, 1669 (2003).
[20] E = S; (a) V.K. Jain, R.P. Patel, V. Venkatasubramanian. *Polyhedron*, **10**, 851 (1991); (b) V.K. Jain, L. Jain. *Coord. Chem. Rev.*, **249**, 3075 (2005); E = Se; (c) L.B. Kumbhare, V.K. Jain, P.P. Phadnis, M.J. Nethaji. *J. Organomet. Chem.*, **692**, 1546 (2007); E = Te; (d) V.K. Jain, S. Kannan, R. Bohra. *Polyhedron*, **11**, 1551 (1992).
[21] (a) E. Alonso, J. Forniés, C. Fortuño, M. Tomás. *J. Chem. Soc., Dalton Trans.*, 3777 (1995); (b) F.D. Rochon, R. Melanson, A. Morneau. *Mag. Res. Chem.*, **30**, 697 (1992); (c) T.G. Appleton, J.R. Hall, S.F. Ralph, C.S.M. Thompson. *Inorg. Chem.*, **28**, 1989 (1989); (d) H.C. Clark, A.B. Goel. *J. Organomet. Chem.*, **178**, C27 (1979); (e) R.A. Plowman, L.F. Power. *Aust. J. Chem.*, **24**, 303 (1971).
[22] J. Ruiz, N. Cutillas, J. Sampedro, G. López, J.A. Hermoso, M. Martínez-Ripoll. *J. Organomet. Chem.*, **526**, 67 (1996).
[23] G. Aullón, G. Ujaque, A. Lledós, S. Alvarez. *Chem. Eur. J.*, **5**, 1391 (1999).
[24] Other planar structures in this class (planar implies a $>170^\circ$ angle between the two square planes). (a) N.D. Ghavale, S. Dey, V.K. Jain, M. Nethaji. *Inorg. Chim. Acta*, **361**, 2462 (2008); (b) R. Oilunkaniemi, R.S. Laitinen, M.S. Hannu-Kuure, M. Ahlgrén. *J. Organomet. Chem.*, **678**, 95 (2003); (c) E.M. Padilla, H.A. Golen, P.N. Richmann, C.M. Jensen. *Polyhedron*, **10**, 1343 (1991).
[25] A. Singh, U. Anandhi, M.A. Cinellu, P.R. Sharp. *Dalton Trans.*, 2314 (2008).
[26] T.J. Williams, A.J.M. Caffyn, N. Hazari, P.F. Oblad, J.A. Labinger, J.E. Bercaw. *J. Am. Chem. Soc.*, **130**, 2418 (2008).
[27] Structures with a bending angle $>165^\circ$: (a) P.A. Koz'min, T.N. Fedotova, G.N. Kuznetsova, M.D. Surazhskaya, I.B. Baranovskii. *Russ. J. Inorg. Chem.*, **36**, 1679 (1997); (b) U. Fekl, R. van Eldik. *Eur. J. Inorg. Chem.*, 389 (1998); (c) R.-D. Schnebeck, E. Freisinger, B. Lippert. *Eur. J. Inorg. Chem.*, 1193 (2000); (d) J. Yoo, Y.-K. Han, Y.S. Lee, Y. Do. *Polyhedron*, **21**, 715 (2002); (e) A.N. Vedernikov, S.A. Binfield, P.Y. Zavalij, J.R. Khusnutdinova. *J. Am. Chem. Soc.*, **128**, 82 (2006).
[28] F. Zhang, E.M. Prokopchuk, M.E. Broczkowski, M.C. Jennings, R.J. Puddephatt. *Organometallics*, **25**, 1583 (2006).
[29] U. Fekl, R. van Eldik, C. Richardson, W.T. Robinson. *Inorg. Chem.*, **40**, 3247 (2001).
[30] This structure also shows H-bonding between the bridging O*H* groups and the triflate anions, although each O*H* H-bonds to only one O atom of different triflate anions. Additionally, the F-atoms of the triflate anions point into the bowl formed by the bent square planes of a neighboring molecule, perhaps providing electrostatic interactions which may also contribute to bending.
[31] *SMART and SAINT Area-detector Control and Integration Software*, Siemens Analytical X-ray Instruments Inc., Madison, WI (1993, 1995).
[32] A. Altomare, G. Cascarano, C. Giacovazzo, A. Guagliardi, M.C. Burla, G. Polidori, M. Camalli. *J. Appl. Cryst.*, **27**, 435 (1994).
[33] P.W. Betteridge, J.R. Carruthers, R.I. Cooper, K. Prout, D.J. Watkin. *J. Appl. Cryst.*, **36**, 1487 (2003).